

Optimising PTO Parameters for Arrays of Wave Energy Converters

Connie Pyromallis

June 3, 2016

1 Introduction

The ocean is a natural source of wave energy, and covers 71% of the Earth's surface, yet it is a relatively untapped source of renewable energy [1, 2]. Wave energy can be harnessed and turned into electricity using a wave energy converter (WEC), of which there are many types. One such type of WEC is a point absorber buoy, which either floats on, or just below, the surface of the water, and moves with the waves to generate energy [3].

Carnegie Wave Energy developed a point absorber called CETO 5. CETO 5 is a fully submerged buoy tethered to the hydraulic pump in a power take off system (PTO) on the sea floor [3, 4]. The up and down movement of waves causes the buoys to move up and down, which in turn drives the pump. The pump pressurises the water in a pipe which spans the distance from the buoys to the shore. When the water reaches the shore, it is either used to turn the turbines of an off the shelf generator to produce electricity, or to power a reverse osmosis desalination to create potable water [5]. A visual representation of this system can be seen in figure 1.



Figure 1: Operation of the CETO system [5].

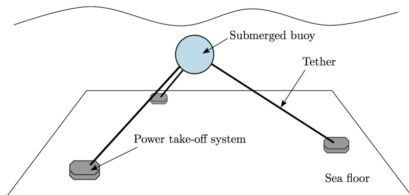


Figure 2: Representation of a three-tether WEC [7].

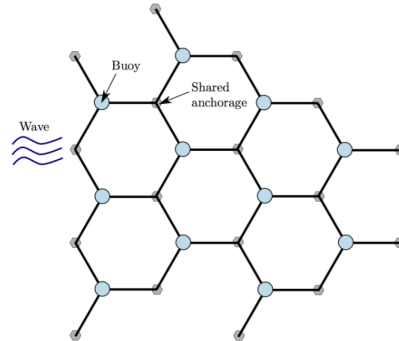


Figure 3: Bird's eye view of array with shared PTO [7].

An alternative to the single-tether buoys are three-tether buoys (depicted in figure 2), in which there are 3 PTOs on the sea floor which each have a tether that connects to the buoy. This allows not only up and down movement (heave) to be captured and converted, but also surge and sway movement [6]. A single buoy can only produce a limited amount of electricity, so they are often deployed in large numbers as an array. In the case of three-tether buoys, PTO can be shared by multiple buoys (see figure 3).

The amount of power absorbed from an incoming wave is maximal if the frequency of the wave matches the natural frequency of the buoy [8]. Thus, we should force the buoy's natural frequency to match the wave's frequency. In addition to containing the hydraulic pump, the PTO also contains a spring with spring constant k (in N/m/s), and damper (decreases amplitude) with damping factor d (in N/m). The natural frequency of the buoy is dependent on d and k , and thus we can control the buoy's natural frequency. Additionally, to avoid damage, tether elongation cannot exceed 3 metres more than its natural length at the boundary between taut and slack. This can be controlled by d . It is important to note that for inconsistent sea states, there will be different wave frequencies, so for constant spring and damper values, the natural frequency will only match with one frequency of waves.

The primary purpose of WEC arrays is to capture energy, and thus it is something researchers aim to optimise. There are many aspects that can be individually optimised, but the key ones are the geometry of the buoy, the control via PTO, and the placement of buoys relative to one another. Our research focus will be control via PTO.

2 Related Work

In an array of buoys, waves will be reflected off of buoys in various directions. This means that constructive and destructive interference can occur, and thus,

in some locations within the array, energy absorption will be increased. This is the reason optimisation of placement of buoys is useful. Previous research into this area includes the development of a model for three-tether buoys in an array and the amount of energy it absorbs. This model is used as a fitness function for various genetic algorithms including (1+1)EA and CMA-ES which mutate the array by moving a single buoy [7].

Optimisation of control for a single buoy is intriguing, because in order to absorb maximum energy in inconsistent seas, the buoy must somehow have knowledge of incoming wave frequencies, in order to alter the natural frequency. Simple gradient-ascent algorithms have been used to alter PTO settings to match the incoming wave [10].

3 Contribution

Using the model for a 3-tether CETO 5 given in [7], we can calculate the power absorbed by each buoy, as well as the total power absorbed, for various array settings and sea states. In our case, we want to vary the PTO settings, d and k , for each buoy, in order to find some setting that lead to increased power absorption. We keep the rest of the variables constant, including: radius of each buoy at 5m, number of rows of buoys at 2, number of buoys per row at 2, distance between each row at 46.669m, and distance between buoys within a row at 53.8888m, ocean depth at 30 m, submergence depth of buoys below the surface at 3 m, and the maximum amount that the buoy can stretch its tethers from slack at 3 m. Note that there are 4 buoys in total, arranged in a diamond shape. Throughout this paper, the bottom-left, top-left, bottom-right, top-right positions of buoys will be referred to as 1, 2, 3, 4 respectively. The frequency of the incoming wave was 0.7 rad/s. We chose this frequency since it is the dominant frequency in the sea state of an area near Sydney (same as the sea state used in [7]).

For an isolated buoy, the optimal PTO settings d and k , for these constants were calculated to be $d=131950$ N/m/s, $k=280350$ N/m which resulted in a total power absorption of 505070 Watts. Throughout this paper, these PTO settings will be referred to as $OPT_{isolated}$. Applying $OPT_{isolated}$ to all buoys in the 2x2 array defined above gives a total power absorption of 1800700 Watts. The power absorptions of each buoy individually can be seen in table 1 (see figure 4 for visualisation). This is our baseline, and the PTO settings which we intend to improve upon.

All of our optimisations were achieved using various grid searches, by considering a valid set of d and a valid set of k , calculating the resulting power for every d and for every k , and maintaining the maximum power, and PTO settings that achieved it. The valid set of d , or k , can be defined by a lower and upper bound for each, and a step size for the difference between each d/k in the set. The grid to search can thus be defined by the lower d and k , upper d and k , and the step size. If D and K are the total number of valid d and k in each set, then the grid search takes $O(DK)$ time to execute.

| Buoy position | Power absorption (Watts) |
|---------------|--------------------------|
| 1 | 428780 |
| 2 | 373280 |
| 3 | 501220 |
| 4 | 497430 |

Table 1: Power absorptions of each buoy at a given position, where each buoy has PTO settings $\text{OPT}_{isolated}$.

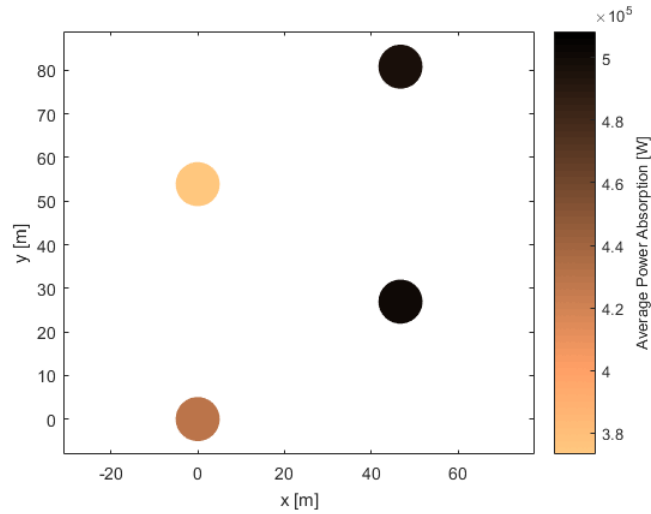


Figure 4: Bird's eye view of buoys, with wave direction from right to left. Shows relative power absorption of buoys, for array in which each buoy has PTO settings $\text{OPT}_{isolated}$. Note that figures 6 and 8 share the same scale for colour to power absorption.

| Buoy position | Power absorption (Watts) |
|---------------|--------------------------|
| 1 | 434480 |
| 2 | 434480 |
| 3 | 509080 |
| 4 | 505180 |

Table 2: Power absorptions of each buoy at a given position, where each buoy has PTO settings found by optimisation 1.

Running one grid search at a high resolution (small step size) for some bounds of d and k was taking too long for our needs (small step size \Rightarrow larger D and K). Instead, we ran a low resolution grid search, and zoomed in on an area of interest to run another. So, we ran successive grid searches, initially starting at the broadest range of d and k bounds with a large step size, and successive searches decreasing step size, and narrowing the upper and lower bounds. We call this approach zooming grid search. In our case, we are trying to find the maximum power absorption, so our area of interest to zoom into, is the location where the maximum is likely to occur. Thus, we centre succeeding grid searches on the maximum of the previous grid search. For the first grid search, the grid needs to be specified. Successive grid searches decrease the step size by a factor of 10, and the lower bounds are the PTO that gave the previous maximum subtract the previous step size, and add the previous step size for the upper bounds. Grid searches continue being executed until the step size is less than 100, which was deemed sufficient by a domain expert.

We took multiple approaches to optimise PTO using grid searches, and each approach will be explained in the following subsections.

3.1 Optimisation 1: Consistent PTO across Buoys

The first approach to was to run a zooming grid search on d and k , where d and k are the PTO settings for all buoys. That is, all buoys have the same PTO settings. The initial grid was: $lower_d = 0$, $upper_d = 400000$, $lower_k = 0$, $upper_k = 550000$, $step = 500000$. The maximum power found by the grid search, and corresponding PTO were: $power=1825100$ Watts, $d=129600$ N/m, $k=279400$ N/m/s. This is a 1.36% improvement to $OPT_{isolated}$. The power absorption of each buoy can be seen in table 2.

3.2 Optimisation 2: Focusing on PTO of an Individual Bouy

In the second approach, we initialised the PTO for all buoys, to $OPT_{isolated}$, and picked one of the buoys in the array, to run a grid search on that buoy's d and k , while the others' stay the same. The initial grid was the same as in optimisation 1.

Optimising buoy 2 in a 2x2 array achieved the greatest power (1855800

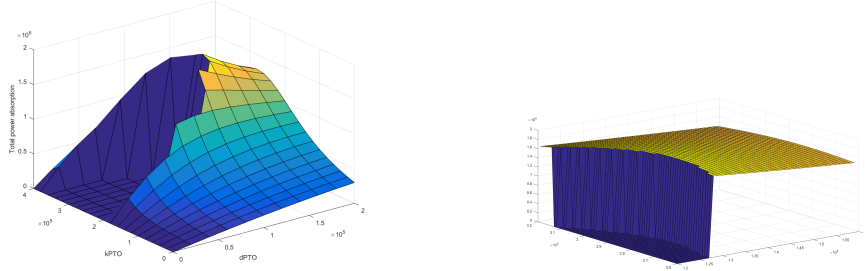


Figure 5: All d and k investigated by a low (left) and high (right) resolution grid search for d and k (same for all buoys), and the resulting powers in the third dimension. These are not the exact grids searched to get the results obtained (different step sizes), but examples for visualisation purposes. The invalid valley is caused by the movement of the buoy exceeding 3m.

| Buoy position | d (N/m/s) | k (N/m) | Total power absorption (Watts) |
|---------------|-------------|-----------|--------------------------------|
| 1 | 118000 | 276300 | 1842500 |
| 2 | 111100 | 271000 | 1855800 |
| 3 | 129100 | 289100 | 1807100 |
| 4 | 128100 | 270700 | 1809800 |

Table 3: Optimal PTO for buoy in given position, and corresponding total power absorptions, resulting from optimisation 2.

Watts) compared to optimising the other buoys (see table 3 for PTO that achieved this, as well as PTO and power absorptions of the other 3 buoys). This is a 3.06% improvement upon $OPT_{isolated}$. A visualisation of the buoys is depicted in figure 6.

3.3 Optimisation 3: Optimising Multiple Individual Buoys Successively

In the third optimisation, the first step was to initialise all PTO to $OPT_{isolated}$. For an ordering of the buoys starting at buoy i (from buoy i to n then 1 to $i-1$), each buoy in that order was optimised, using optimisation 2. We continuously cycled through that order and optimised until no improvement was made after $n-1$ consecutive optimisations (where n is the number of buoys). Note that in each iteration of optimisation, the PTO for each buoy are maintained, so that the next optimisation finds the optimal power, considering the previously calculated PTO for other buoys. The buoy optimised in the i th iteration will be the $(i-1)\%n+1$ buoy in the order, with the 0th optimisation iteration corresponding to all PTO initialised to $OPT_{isolated}$.

The optimisation of single buoy was done by using an algorithm similar to optimisation 2, except, instead of initialising everything to $OPT_{isolated}$, we use

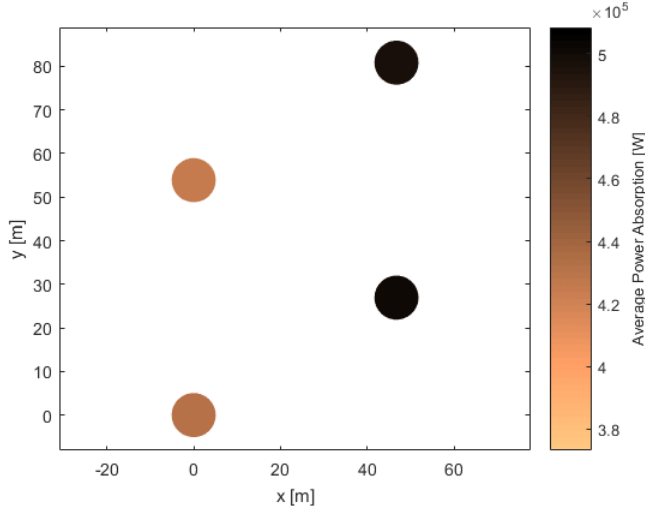


Figure 6: Relative power absorptions of buoys with PTO found in optimisation 2 by optimising buoy 2.

the previously calculated PTO. In addition, to save time, when doing the zoom for the grid search, the initial grid has a step size of 5000, and is bounded by $\pm 20\%$ of the previous optimal d and k that have been calculated for that buoy e.g., during the first optimisation of a buoy, lower bound will be $0.8 * OPT_{isolated}$, upper will be $1.2 * OPT_{isolated}$. This means that the grid search has to zoom in fewer times.

The order that produced the best power was 2341, with: power=1913800, $d=[128560, 118350, 111160, 130060]$, $k=[275280, 278220, 275200, 283280]$ (ith element of d and k corresponds to ith buoy). See figure 8 for visualisation. The improvement percentage upon $OPT_{isolated}$ was 6.014%. The amount of power absorption after each iteration when optimising order 2341 has been graphed in figure 7. The optimal d and k , and corresponding powers for the other orders can be seen in table 4.

4 Discussion

All experiments were run on a single intel i5 core. The amount of time taken for the model to determine the power absorption of a 2×2 array (with array settings given in the beginning of section 3) on average was 2.187 seconds (based on 100 samples). The computation time of the model is independent of the PTO settings for each buoy, so using different PTO should still take similar times to compute. Recall that the number of model calculations made by a grid search is DK . Optimisation 1 required one zooming grid search. Given the initial grid, 3 grid searches in total will be run, and the model will calculate the power

| Order | d ₁ | d ₂ | d ₃ | d ₄ | k ₁ | k ₂ | k ₃ | k ₄ | Power |
|-------|----------------|----------------|----------------|----------------|----------------|----------------|----------------|----------------|---------|
| 1234 | 117450 | 110850 | 130060 | 128560 | 276420 | 289720 | 283280 | 276280 | 1911100 |
| 2341 | 118350 | 111160 | 130060 | 128560 | 278220 | 275200 | 283280 | 275280 | 1913800 |
| 3412 | 115060 | 129450 | 129560 | 128250 | 260780 | 276720 | 284280 | 278520 | 1857500 |
| 4123 | 118560 | 111060 | 131950 | 128560 | 278780 | 274780 | 280350 | 274280 | 1908100 |
| 4321 | 131950 | 110560 | 129560 | 128560 | 280350 | 269280 | 287280 | 274280 | 1870900 |
| 3214 | 130060 | 110560 | 129560 | 131950 | 278280 | 267780 | 284280 | 280350 | 1865700 |
| 2143 | 118350 | 111450 | 130060 | 129060 | 278520 | 276120 | 283780 | 280280 | 1911800 |
| 1432 | 117450 | 111060 | 130060 | 129060 | 278420 | 289280 | 283780 | 279780 | 1909800 |

Table 4: Optimal PTO for each buoy, and corresponding total power absorptions, resulting from optimisation 3, where d_i and k_i are d and k of i th buoy in N/m/s and N/m respectively.

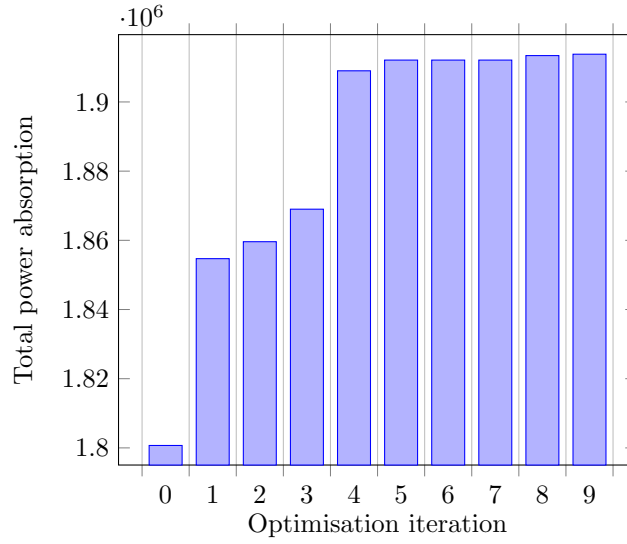


Figure 7: Total power absorptions at the i th optimisation iteration for order 2341. The 4th optimisation iteration occurred when buoy 1 was optimised.

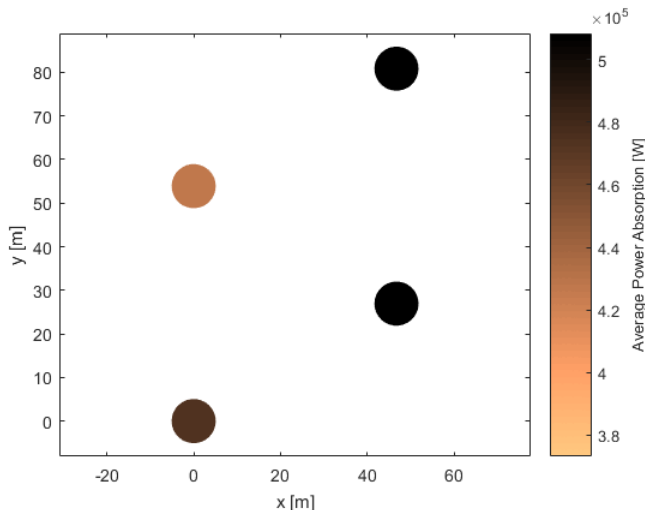


Figure 8: Relative power absorptions after optimisation 3 on order 2341. Notice that the colours for each buoy in this plot are significantly darker than those in figure 4.

absorption a total of 990 times. Thus, optimisation 1 takes 2165 seconds (36.1 minutes) to run. Same computation time also applies to optimisation 2 for each buoy position, as each uses a zooming grid search with the same initial grid as in optimisation 1. Optimisation 3 uses a different initial grid for each optimisation of each buoy. In addition, the number of optimisations of an individual buoy in optimisation 3 varies for each order. The total number of model calculations, and computation time can be seen in table 5.

In regards to optimisation 2, it is conceivable that optimising buoy 2 achieved the greatest power absorption compared to optimising the other buoys, because it has the lowest power absorption of all the buoys in the baseline, and thus has the most potential for improvement. Additionally, more wave interaction occurs as you move further to the back of the array (back meaning furthest away from source of waves), since more waves have been bounced by the buoys. Since buoy 2 is right behind the two buoys in the first row, it will likely experience the most varied waves that $OPT_{isolated}$ is least optimal for. The same logic can be applied to buoy 1 and 2 in optimisation 3, (notice the spikes in total power in figure 7). However, it is not clear why having these buoys be the first in the order to optimise, results in the greatest total power absorption.

Though zooming when executing the grid search gives a significant speed up in computation time, one of the limitations of it is that it can zoom into the wrong place i.e., zooming grid search may not find the same optimum as one high resolution grid search over the same bounds. Consider figure 5 on the left. It appears that the maximum power would occur at the apex of the invalid region. A side view of this figure has been provided in figure 9, so that we can

| Order | # of individual buoy optimisations | # of model calculations | Computation time (s) | Computation time (hrs) |
|-------|------------------------------------|-------------------------|----------------------|------------------------|
| 1234 | 9 | 6300 | 13778.1 | 3.83 |
| 2341 | 12 | 8371 | 18307.4 | 5.09 |
| 3412 | 11 | 7725 | 16894.6 | 4.69 |
| 4123 | 6 | 4208 | 9202.9 | 2.56 |
| 4321 | 6 | 4243 | 9279.4 | 2.58 |
| 3214 | 6 | 4220 | 9229.1 | 2.56 |
| 2143 | 9 | 6290 | 13756.2 | 3.82 |
| 1432 | 8 | 6529 | 14278.9 | 3.97 |

Table 5: The number of optimisations of individual buoys, number of model calculations, and computation time of using optimisation 3 on a given ordering of buoys.

see d vary, but only the maximum power across all k , for each d . This confirms that the maximum does indeed occur at the apex ($d=140000$, $k=280000$). Now consider the same bounds with a step size of double the current one. This means that the search will consider $d=120000$, but not $d=140000$ where the maximum appears to be. Thus, the maximum for the lower resolution would occur at $d=120000$, $k=240000$, and the successive zoomed in grid search would centre on there. Thus, it appears the actual optimum can be missed by zooming in.

5 Conclusion

The total power absorption of a 2x2 array can be improved by up to 6.014% compared to the baseline where $OPT_{isolated}$ is applied to the PTO of all buoys in the array. This improvement was achieved by iteratively optimising the PTO of individual buoys. Future work on this would involve looking at a wider variety of arrays, with different submergence depths and more buoys, etc. We could also rerun optimisation 2 with initialisation of PTO to the values found in optimisation 1, instead of $OPT_{isolated}$. In addition, we can run optimisation 3 for other orders that are not just clockwise or anti-clockwise.

References

- [1] Drew B, Plummer AR, Sahinkaya MN. *A review of wave energy converter technology*. Proceedings of the Institution of Mechanical Engineers, Part A: Journal of Power and Energy, 223(8). 2009; 887–902.
- [2] Esteban M, Miguel E, David L. *Current developments and future prospects of offshore wind and ocean energy*. Applied Energy. 2012;90: 128–136.

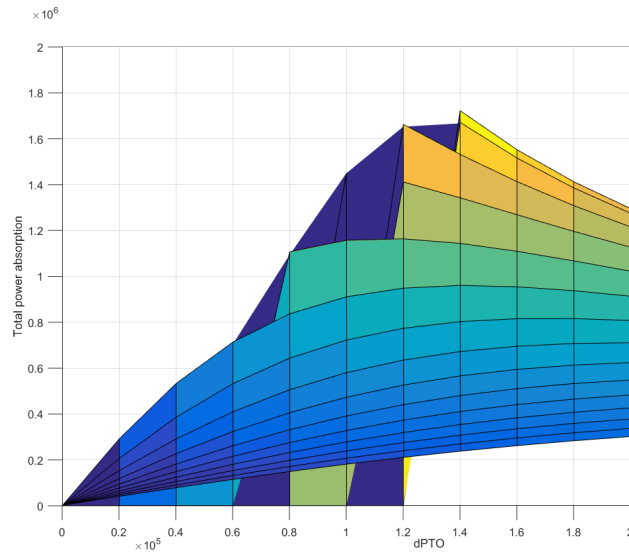


Figure 9: Side view of figure 5.

- [3] Lagoun MS, Benalia A, Benbouzid MEH. *Ocean wave converters: State of the art and current status*. 2010 IEEE International Energy Conference. 2010. doi:10.1109/energycon.2010.5771758.
- [4] Mann LD, Burns A, and Ottaviano M. *CETO, a carbon free wave power energy provider of the future*. In Proceedings of the 7th European Wave and Tidal Energy Conference. 2007.
- [5] Mann LD. *Application of Ocean Observations & Analysis: The CETO Wave Energy Project*. Operational Oceanography in the 21st Century. 2011. pp. 721–729.
- [6] Scruggs JT, Lattanzio SM, Taflanidis AA, Cassidy IL. *Optimal causal control of a wave energy converter in a random sea*. Applied Ocean Research. 2013;42: 1–15.
- [7] Cazzalato BS, Ding B, Neumann F, Sergiienko N, Shekh S, Wagner M, Wu J. *Fast and effective optimisation of arrays of submerged wave energy converters*. Accepted by GECCO. 2016.
- [8] Falnes J. *Ocean Waves and Oscillating Systems: Linear Interactions Including Wave-Energy Extraction*. Cambridge University Press. 2002.
- [9] du Plessis J. *A Hydraulic Wave Energy Converter*. Stellenbosch University. 2012.

- [10] Ding B, Cazzolato BS, Arjomandi M, Hardy P. *Sea-state Based Maximum Power Point Tracking Damping Control of a Fully Submerged Oscillating Buoy*. Under review by Journal of Ocean Engineering. 2016.